

# The Miniball Cluster

Note that this documentation refers to the old cryostats. So some parts are out of date! The encapsulation, Doppler correction, segmentation and pulse-shape analysis sections should still be the same, but the feedthroughs, preamplifiers and mounting has changed.

## Contents

<b>1</b>	<b>2022 upgrade</b>	<b>2</b>
<b>2</b>	<b>Encapsulation</b>	<b>2</b>
<b>3</b>	<b>Doppler correction</b>	<b>2</b>
<b>4</b>	<b>Segmentation</b>	<b>4</b>
<b>5</b>	<b>Pulse-shape analysis</b>	<b>6</b>
5.1	Segment hit pattern . . . . .	7
5.2	Radial information . . . . .	7
5.3	Azimuthal information . . . . .	9
5.4	Position sensitivity . . . . .	10
<b>6</b>	<b>Feedthroughs</b>	<b>11</b>
<b>7</b>	<b>Preamplifiers</b>	<b>11</b>
<b>8</b>	<b>Mounting</b>	<b>12</b>

---

<sup>1</sup>Nigel Warr October 2022

## 1 2022 upgrade

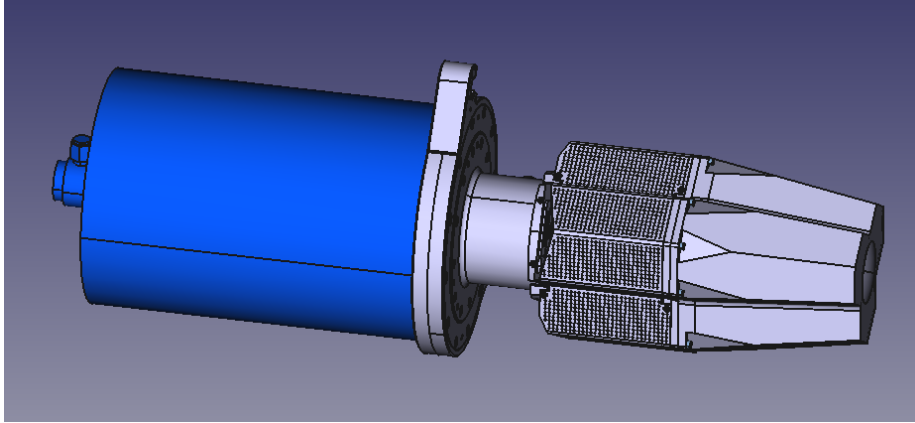


Figure 1: The new Miniball triple cryostat (2022)

In 2022 the cryostats were upgraded. The same capsules are used inside, but AGATA preamplifiers are used now. These have differential outputs via MDR cables. One MDR cable is used for the core and one for the six segments (compared to AGATA, where there is one for the core and six for the 36 segments). One of the new cryostats is shown in figure 1.

## 2 Encapsulation

The Miniball detectors are encapsulated, like the Euroball detectors. This means that the Ge crystal is housed inside a thin aluminium can which is sealed by Eurysis at Jülich, before they are delivered.

This means that it is possible to have the encapsulated detectors out in the air and to handle them, which would otherwise not be possible. Given the complexity of the Miniball detectors, this has proved essential for maintenance

There is a slight loss of efficiency at low energy due to the aluminium can, but this effect is negligible for realistic applications.

## 3 Doppler correction

Miniball is designed for use with radioactive beam experiments, where the nuclei we want to study are the beam particles, not the target ones. Consequently, they are moving with  $v/c$  values of a few percent. This causes a significant Doppler shift, and since the detectors subtend a finite solid angle, the energy of a  $\gamma$  ray detected in different parts of the detector will be different, even if the unshifted energy is the same, leading to a Doppler broadening.

In order to overcome this problem, two techniques are used:

- Segmentation of the outer electrode, to divide up the crystal into parts, so the Doppler correction can be performed separately for each part.

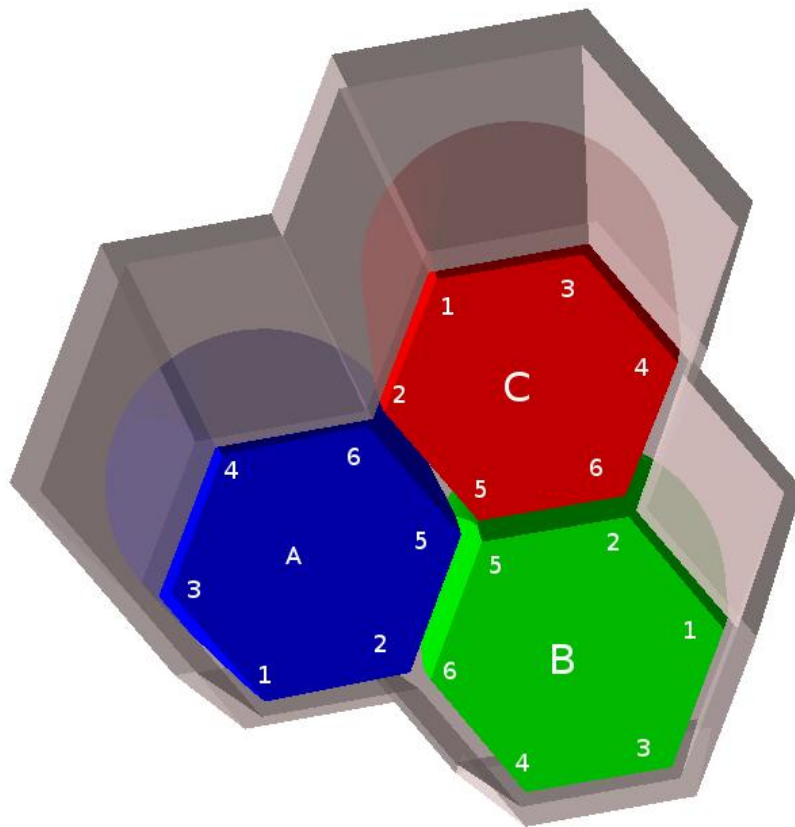


Figure 2: The numbering of the segments. Note that segment 5 is always in the centre of the cluster. The order is determined by the pins on the capsule, so it does not follow a logical geometric pattern. In 2022 the prototype of a new capsule design was tried out in MB10081C and it has a logical (clockwise) ordering with segment 6 in the middle.

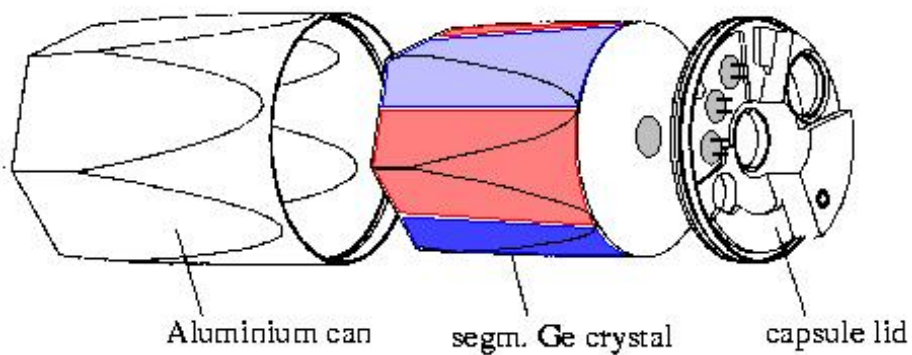


Figure 3: Encapsulation

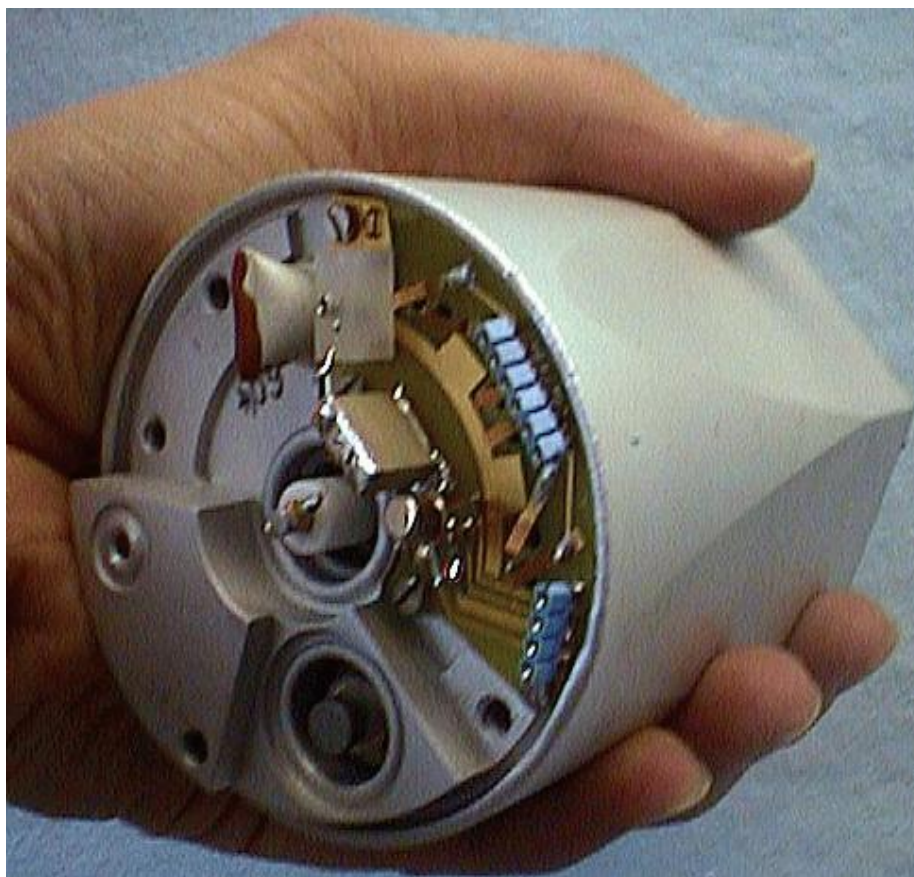


Figure 4: The capsule containing the segmented HPGe crystal. Note that one of the old preamplifiers is mounted on the top. These have been replaced by the AGATA type of preamplifier.

- Pulse-shape analysis: the shape of the pulse can be shown to depend on the position of the interaction in the crystal. We use this pulse shape to try and determine the position.

## 4 Segmentation

A conventional Ge detector has a quasi-cylindrical geometry with one outer electrode and one central “core” electrode. High voltage is applied to the core electrode. The core electrode doesn’t quite go to the front face, because wherever the core reaches a face, it is necessary to passivate the surface because of the high voltage on the electrode. This passivation leads to a dead layer. Consequently, in a conventional detector, the electrode only reaches the surface at the back of the crystal, where the dead layer isn’t a problem, and at the front, the core doesn’t reach the front surface. Then we can either read out the outer electrode via a DC-coupled field effect transistor (FET) or the core electrode via an AC-coupled FET.

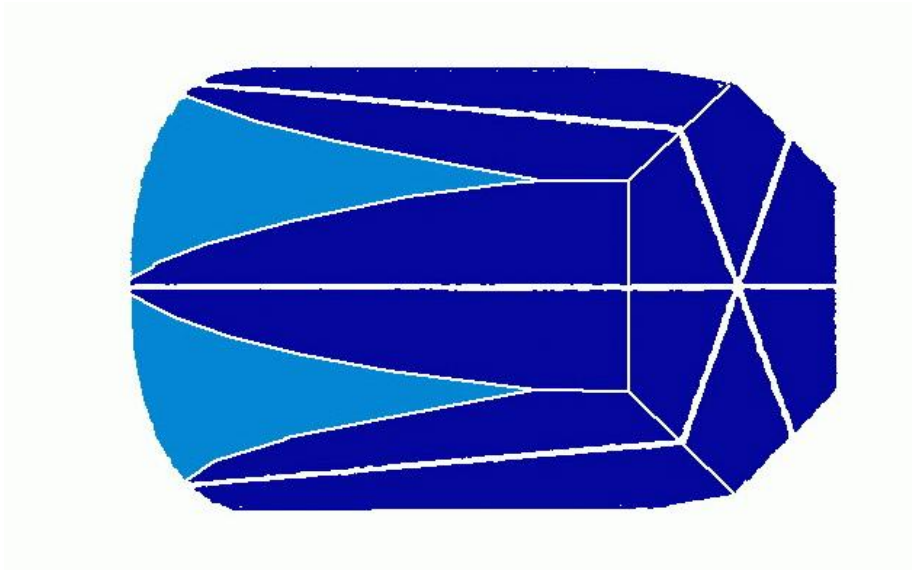


Figure 5: The 6-fold segmented Miniball crystals

This is the same for a Miniball detector, except that the outer electrode is cut into six longitudinal slices, each of which has its own DC-coupled FET readout. Furthermore, we read out the core signal using an AC-coupled FET. See figure 6.

When a  $\gamma$  ray is completely absorbed via the photoelectric effect in the Ge crystal, electron and hole pairs are produced. The electrons migrate to the core (which for Miniball detectors is under positive high voltage) and the holes migrate to the nearest segment of the outer electrode. Both the segment and the core electrodes see the full energy of the  $\gamma$  ray.

If, however, a  $\gamma$  ray is scattered inelastically and then absorbed, there are two interaction points in the crystal, which may be in different segments. The core electrode will still see all the electrons, corresponding to the full  $\gamma$ -ray energy. For the segments, on the other hand, the holes produced at the first interaction point will go to one segment electrode, while the holes produced at the other interaction point go to the other electrode. Consequently, each segment electrode sees only part of the  $\gamma$ -ray energy. In principle, we can obtain the full energy, by adding up the energies measured on the segments, or by simply looking at the core energy. These two methods should give the same result, except that the error on the sum of several segments will be greater than the error on the core.

What we need, in order to perform the Doppler correction is the position of the first interaction, but what we obtain is the energy deposited in each segment by the interactions. There may be two interactions in one segment, giving us the sum energy. Also, we don't know which segment was hit first. We use the following principle:

first interaction is assumed to be equivalent to main interaction

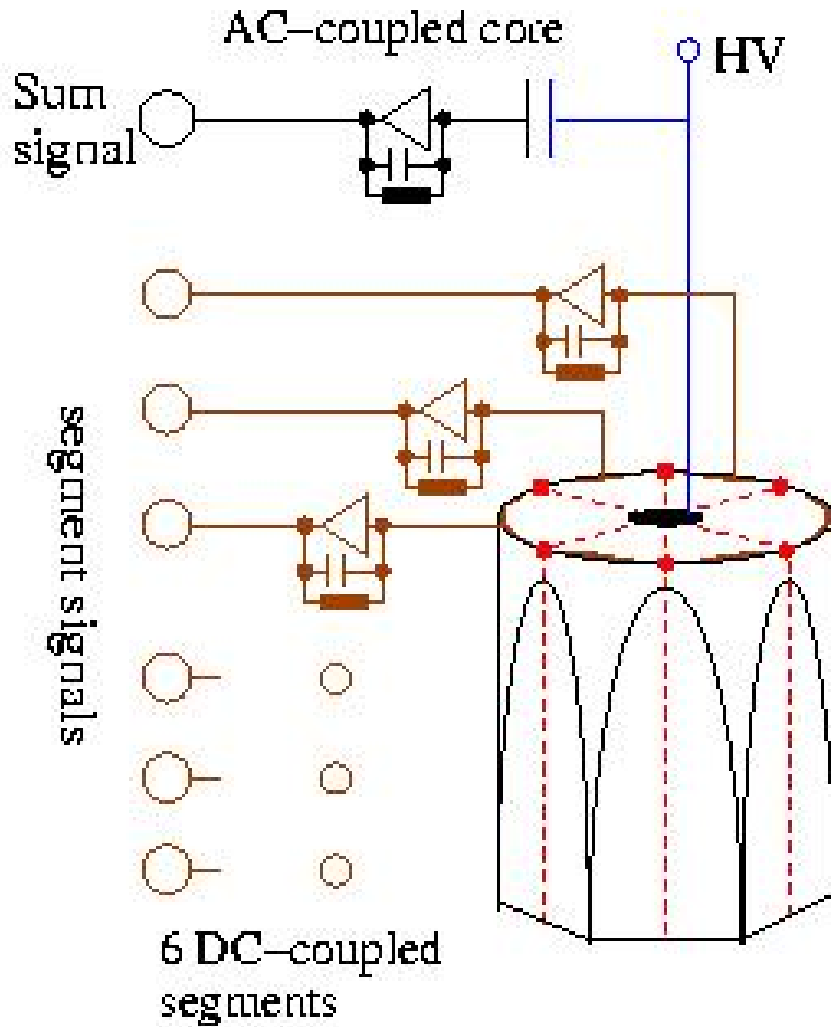


Figure 6: The readout of the Miniball capsule

This means that we assume that the first interaction is either the one which gives the largest energy deposition, or at least it is geometrically close to it. For low-energy and high-energy  $\gamma$ -rays, it is likely that this is true, but for intermediate energies, this assumption is not as good. However, in the absence of full tracking, it is all we have to go on.

## 5 Pulse-shape analysis

The Miniball detector gives us seven signals (core and six segments) for each event. We analyse the shapes of these pulses to obtain position information.

## 5.1 Segment hit pattern

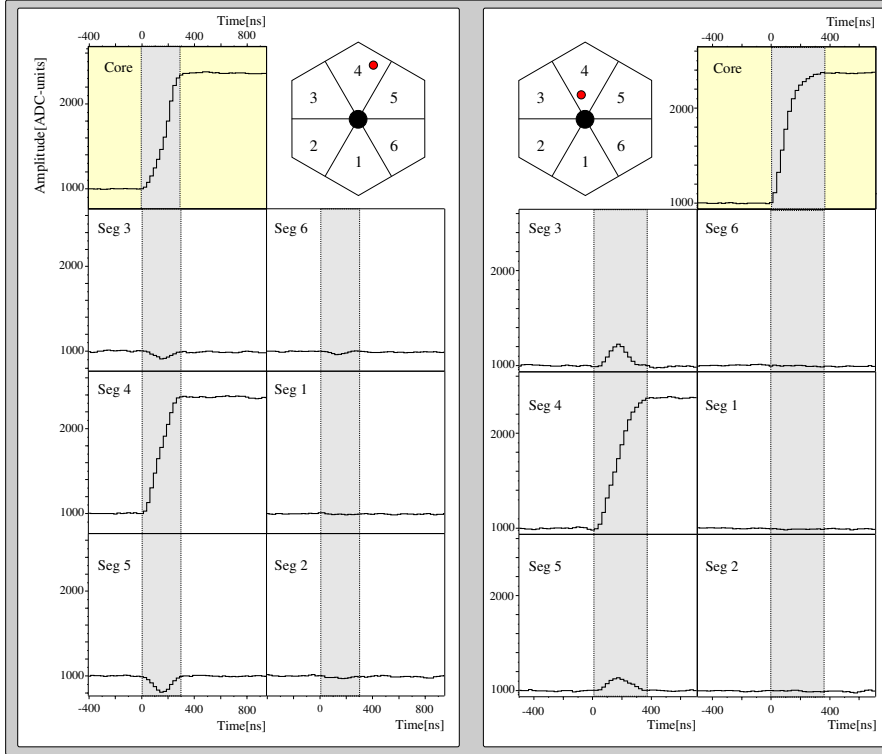


Figure 7: Pulses acquired for interactions in two different parts of segment 4.

Just looking at which segment was hit, and in particular which segment has the greatest energy deposition, allows us to divide the detector into six. This makes it possible to perform a better Doppler correction than if we use the whole capsule.

## 5.2 Radial information

When an interaction occurs in the crystal, electron-hole pairs are produced, which migrate under the influence of the electric field. The electrons go to the core electrode (where we apply positive high voltage) and the holes to the nearest outer segment electrode. The signal we see on the oscilloscope at the output of the preamplifier has a rising flank determined by the time taken for the charge carriers to reach the electrode and a trailing flank which is determined by the characteristics of the preamplifier. This has a nominal decay constant  $\tau = 50 \mu\text{s}$ , though in practise it can vary by about 10 % from the nominal value.

The further the interaction takes place from the core, the longer it takes for the signal on the core to rise. Consequently, we define a quantity referred to as “time to steepest slope”, which is the time for the core signal to reach its steepest gradient (this being the time when the greatest number of charge carriers arrive) and this quantity is dependent on the distance the charge carriers have to travel within the crystal.

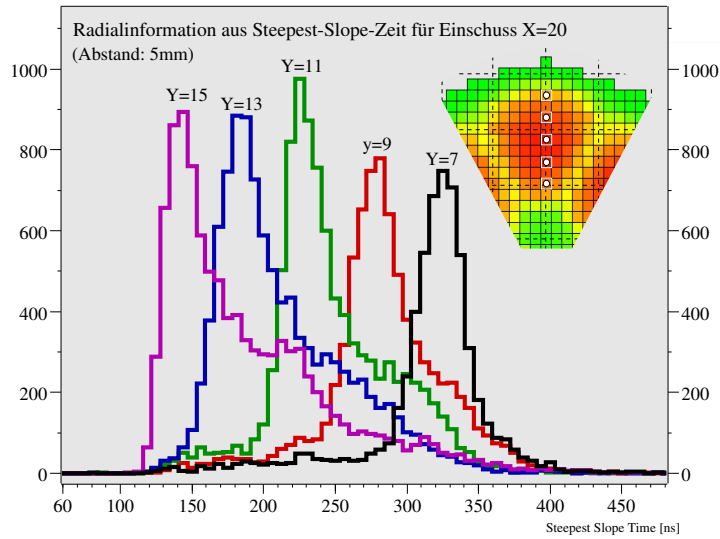


Figure 8: Time to steepest slope for different radial positions (shown in different colours). Note the right tails which are due to the effect of the front end.

For the sake of simplicity, we assume a cylindrical geometry and the time to steepest slope is then proportional to the radius of the interaction. This is a reasonably good approximation for most of the crystal, but is rather poor at the closed front end. Suppose for example, the interaction takes place at zero radius right in the front of the crystal between the front face and the core electrode. There will still be some time for the electrons to move to the core, which will make the radius of interaction appear larger than it really is. Note also, that the distance which the time to steepest slope method measures is not the geometrical distance, but the distance measured along the direction of motion of the electrons, which is determined by the field lines. These field lines are quite curved at the front of the detector.

If we scan a Miniball detector radially using a collimated source (see figure 8) and look at the time to steepest slope, we see a clear correlation between the radial position and the time to steepest slope. We also clearly see the effect of the closed front end which causes  $\gamma$  rays absorbed in the front part of the detector to have greater times to steepest slope than one would get for a perfectly cylindrical geometry. This gives rise to the tails seen in the figure (this was investigated with a 12-fold segmented detector which could separate out the front and back parts).

Note that this technique is not specific to segmented detectors as it only uses the core signal. We normally look at this on the core electrode, though we could also look at segments. For the segments, it is the holes which are the charge carriers and the time to steepest slope is proportional to the time taken for the hole to migrate to the outer electrode, so it is proportional to  $r_{max} - r$ , where  $r_{max}$  is the maximum radius of the crystal and  $r$  is the radius of interaction, not to  $r$ .



### 5.3 Azimuthal information

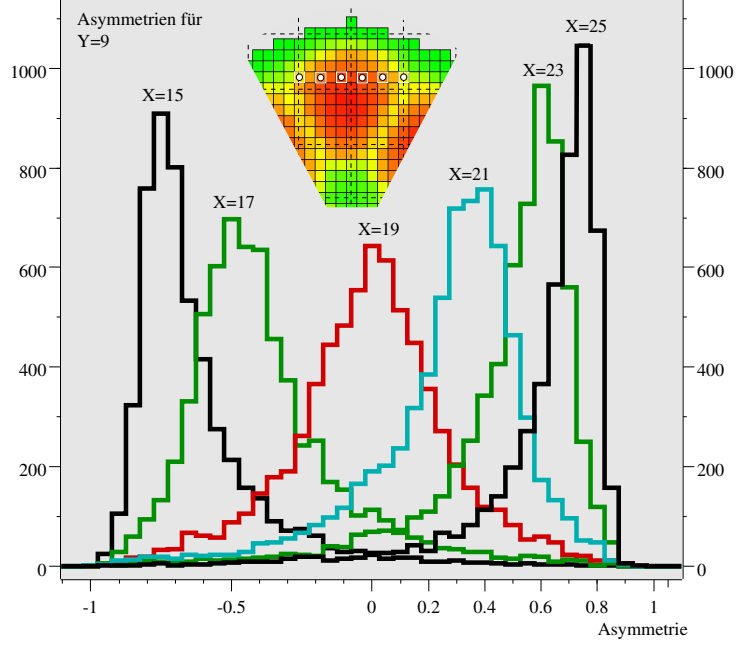


Figure 9: Mirror-charge asymmetry for different azimuthal positions (shown in different colours).

If an interaction occurs near the core electrode, the electrons migrate quickly to that electrode and are absorbed. The holes take a lot longer to reach the outer electrode as it is further away, so for a time there is a net charge imbalance. This net charge imbalance induces mirror charges in the neighbouring segments, the amplitude of which is proportional to the distance to the corresponding segment boundary.

In other words, if an interaction occurs in segment 3 close to the boundary with segment 4, mirror charges will be induced in both segments 2 and 4, but the one in segment 4 will have a significantly larger amplitude.

We define the quantity “mirror-charge asymmetry” to be the mirror charge amplitude on the segment to the left minus that to the right, divided by the sum of the two. This is indicative of the distance to the segment boundary.

Note that if the interaction takes place near the outer edge of the crystal, it is the holes which are absorbed first and the electrons which give rise to a net charge imbalance, so the sign of the mirror charges are inverted. The asymmetry effect is the same, however. Note, though, that events in the middle produce virtually no mirror charge.

In figure 9 we can see the mirror-charge asymmetry for different azimuthal positions.

Asymmetry vs. Steepest-slope time  
for neighbouring segments

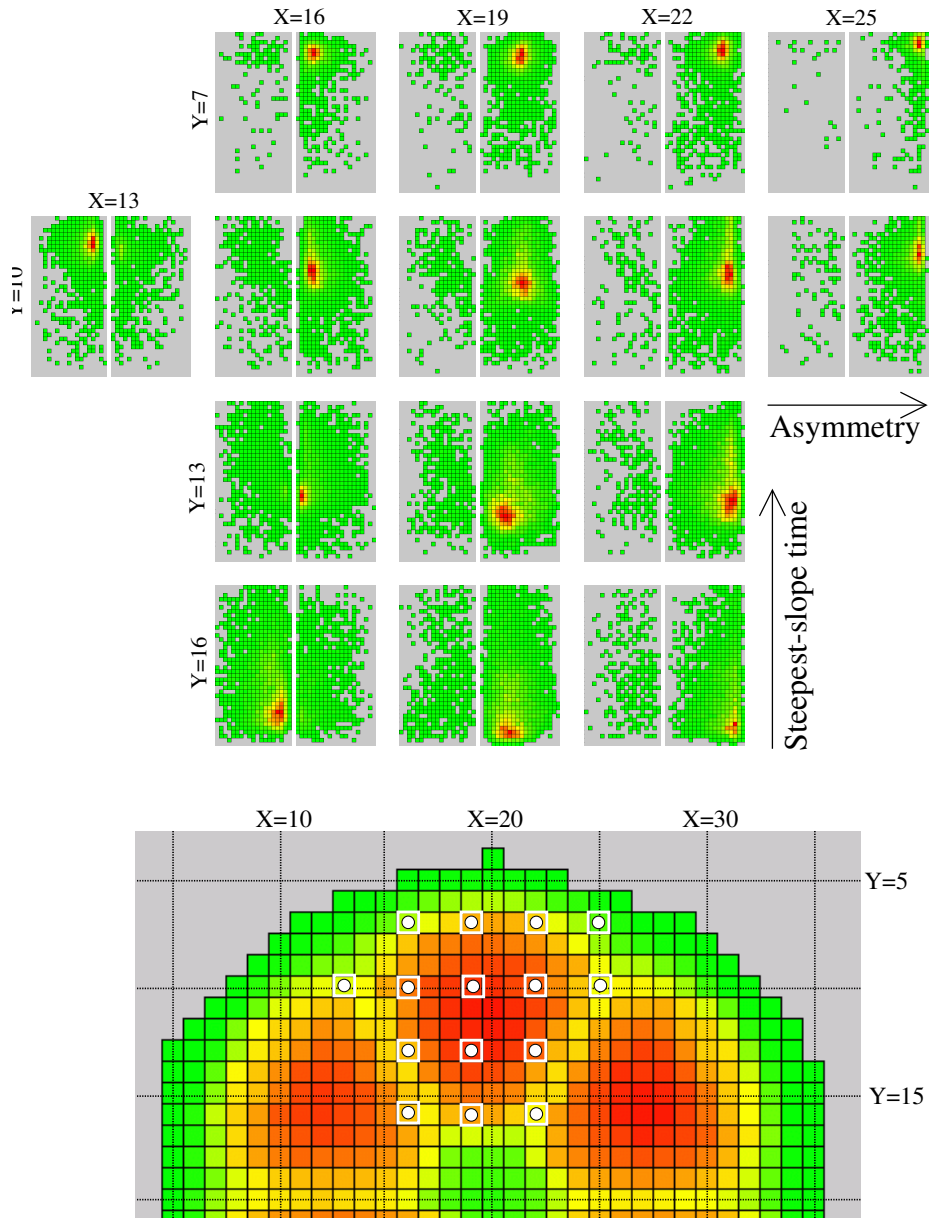


Figure 10: 2-D scan of Miniball detector

#### 5.4 Position sensitivity

Armed with the time to steepest slope and mirror charge asymmetry methods, it has been shown [1] that we can divide a 6-fold segmented Miniball crystal into about a hundred pixels, giving us two orders of magnitude better granularity.

This can be seen on the 2-dimensional scan in figure 10 which was for the 12-fold segmented detector. For several positions in one segment, we show time to steepest slope vs. mirror charge asymmetry.

## 6 Feedthroughs

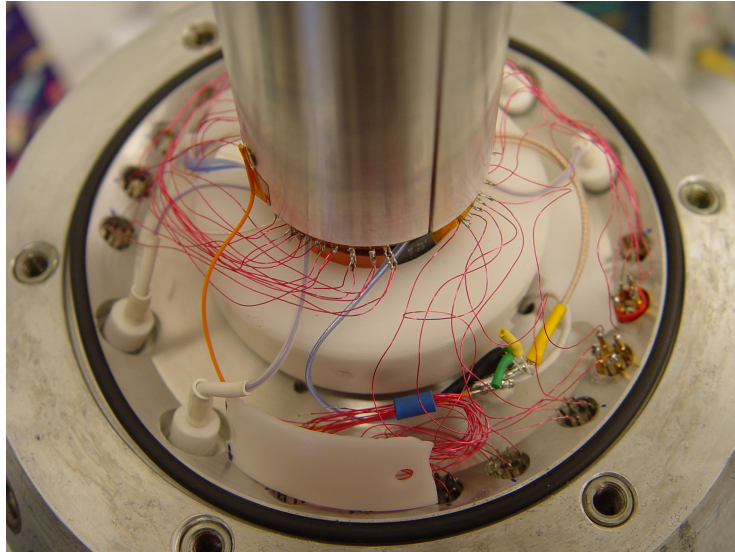


Figure 11: The feedthroughs as seen once the star where the detectors are mounted and the shoulder of the detector are removed. This is out of date.

This section refers to the old cryostats. The new ones are different.

## 7 Preamplifiers

This section refers to the old preamplifiers. The new cryostats are equipped with the AGATA type of preamplifier.

There are two issues concerning the preamplifiers for the Miniball clusters compared to older detectors. Firstly, we now have to have 7 channels per detector, which gives us 21 for a triple cluster and we don't have any more space, so the preamplifiers (both the cold and warm parts) have to be smaller. Secondly, our requirements for pulse-shape analysis mean we need a preamplifier with a greater bandwidth.

Figure 12 shows the cold part of the preamplifier, which is mounted directly onto the capsule and the large white piece on the left is the coupling capacitor. There are six FETs on the outer edge and one more (for the core) attached to the coupling capacitor.

Figures 13 and 14 show the warm part of the preamplifier for a single channel.



Figure 12: The cold part of the preamplifier, with a Euro coin for size comparison. This is out of date.

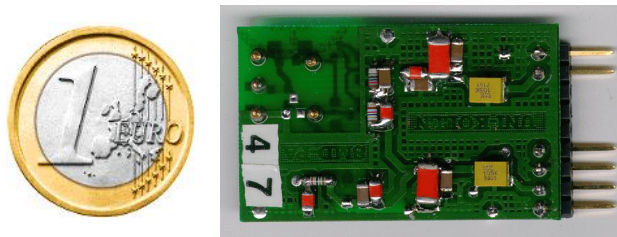


Figure 13: The back of the warm part of the preamplifier, with a Euro coin for size comparison. This is out of date.

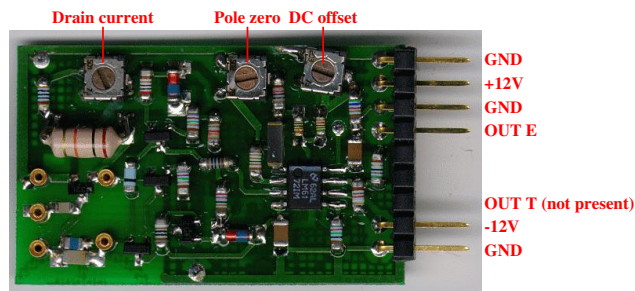


Figure 14: The front of the warm part of the preamplifier. This is out of date.

## 8 Mounting

This section refers to the old cryostats. The new ones are mounted differently.

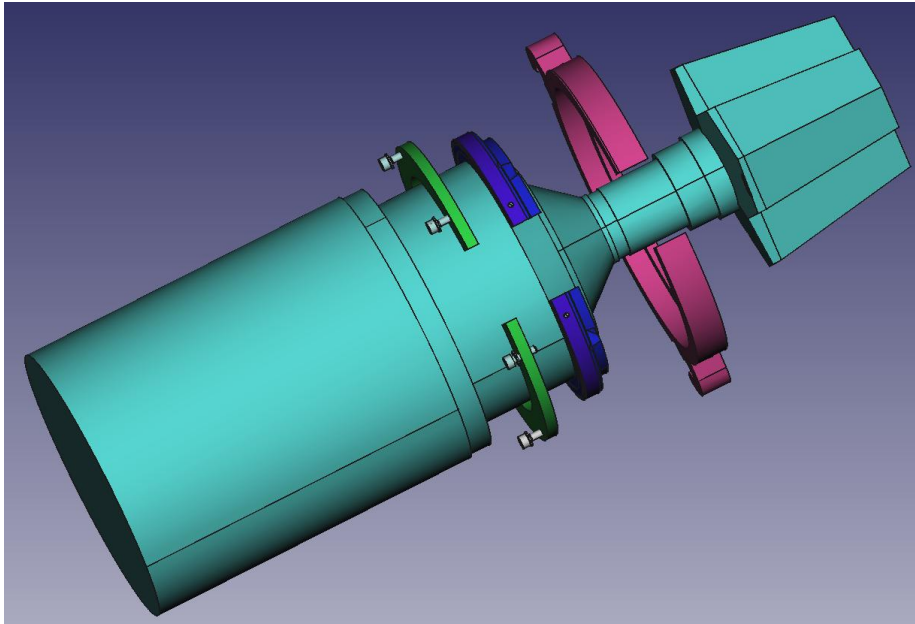


Figure 15: The old cryostat with its mounting rings. The pink ring is part of the frame. When mounted the green part bolts onto the pink part, sandwiching the blue part, which is bolted onto the detector, but can still rotate.

Figure 15 shows the way the cluster is mounted onto the frame. The pink part is part of the frame. The procedure is as follows:

- Put the green part on the detector by passing the neck of the detector through the gap in the green ring.
- Put the blue part on the detector in the same way and bolt it to the detector. Note that the teflon has to be removed to get at the bolts and should then be put back when it is bolted. This blue part has teflon on both faces and at the side.
- The pink part is mounted on the frame and the detector is brought to it so that its neck passes through the gap in the pink ring.
- Then the blue part is inserted into the pink part so that the edges of the blue and pink parts are flush.
- Then the green part can be bolted onto the pink part, so that they sandwich the blue part between them. In this way, the blue part can still rotate freely (the teflon keeps the friction down), but it is held between the pink and green parts.

## References

- [1] D. Weißhaar, PhD thesis.

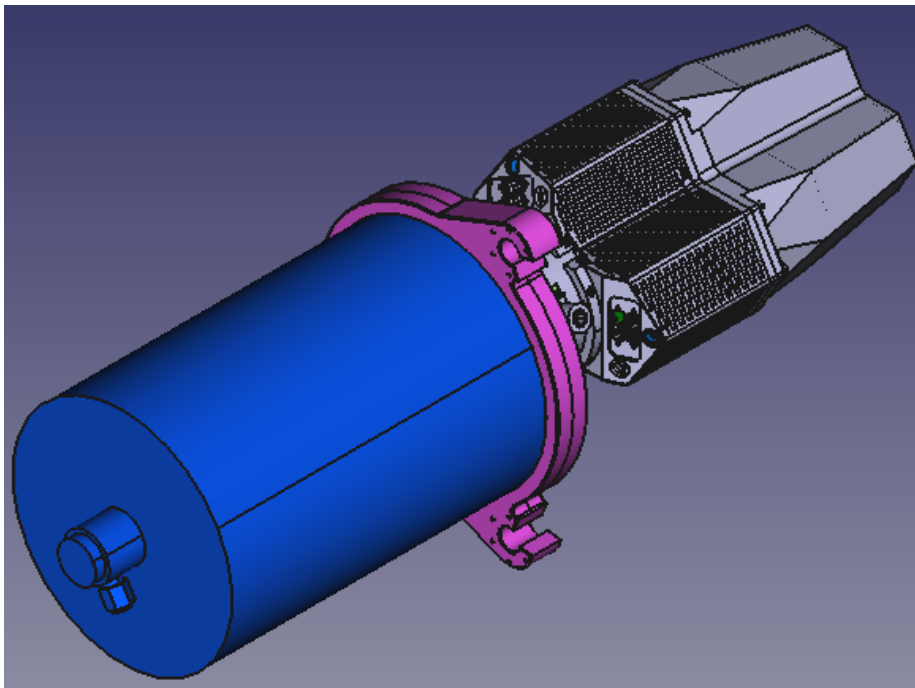


Figure 16: The Miniball cluster with its mounting ring. The pink ring is mounted onto two rods and then fixed. The pink part is equivalent to the pink part of figure 15.